Mol. Cryst. Liq. Cryst., 1997, Vol. 302, pp. 99–110
Reprints available directly from the publisher
Photocopying permitted by license only

LAYER COUPLING FOR MOLECULAR ORIENTATION IN THE FIELD INDUCED ANTIFERROELECTRIC-FERROELECTRIC LIQUID CRYSTAL PHASE TRANSITION

JAE-HOON KIM, JU-HYUN LEE, and SIN-DOO LEE*
Physics Department, Sogang University, C. P. O. Box 1142, Seoul, Korea

Abstract We report on the layer coupling for the electric field induced ferroelectric ordering in antiferroelectric liquid crystals (AFLCs). On approaching the field induced antiferroelectric-ferroelectric (AF-FO) transition, the electro-optic response abruptly increases, reaches a maximum, and then saturates with increasing the electric field. Moreover, the associated switching time exhibits two sharp peaks, indicating the existence of an intermediate ferrielectric-like phase in the middle of the AF-FO transition. The anomaly observed is described in terms of layer coupling in a simplified model which contains interactions of both the nearest (N) and next nearest (NN) neighboring layer pairs. The coupling constants for the N and NN neighboring layers are estimated.

INTRODUCTION

Since the observation of antiferroelectricity in 4 - (1-methylheptyloxycarbonyl) phenyl 4' - octyloxybiphenyl - 4 - carboxylate (MHPOBC), antiferroelectric liquid crystals (AFLCs) have been extensively studied for understanding their physical properties such as thermodynamic, optical, electro-optical, and dielectric properties.[1–6] AFLCs possess a layered structure in which the herringbone formation of the molecular orientation in successive layers undergoes a helical rotation. The molecules arrange themselves in the layers with the molecular long axis inclined at an angle to the layer normal but in the opposite sense in two adjacent layers; the spontaneous polarizations in the neighboring layers point in the opposite sense of the direction perpendicular to the tilting plane, thereby canceled each other.

Although the origin of this novel AFLC structure has not been fully understood yet, it is believed that the pairing of transverse dipole moments in neighboring layers is responsible for the structure.[7,8] In the presence of an external electric field, high enough to overcome the pairing energy, a field induced transition may occur in such a way that an antiferroelectric (AF) phase transforms into a ferroelectric (FO) phase

through an intermediate ferrielectric (FI) phase.[9,10] Based on experimental results, some theoretical descriptions have been made to explain the static and dynamical properties of spatial molecular reorientation during the field induced AF-(FI)-FO transition.[11-14] In most existing theories, the dipole-dipole interactions between the nearest (N) neighboring layers only were taken into account. However, the coupling between the next nearest (NN) neighboring layers is expected to play an essential role in describing the FI phase.

In the present work, we report on an anomaly in the molecular switching process during the electric field induced AF-FO phase transition, which can not be described in a bilayer model.[8] The main features of the AF-FO transition and the anomaly observed in the switching time can be understood in terms of the layer coupling between the NN neighboring layers. The existence of an intermediate FI-like phase in the middle of the AF-FO phase transition is also discussed within an analytical model we developed.

EXPERIMENTAL

We studied a commercial mixture of CS4000, provided from Chisso Petrochemical Co., which has an AF phase at room temperature. The sequence of the liquid crystalline phases of this material, determined self-consistently from photopyroelectric and dielectric measurements,[15] is as follows: I $\rightarrow$ (100 °C) $\rightarrow$ Sm A $\rightarrow$(75.6 °C) $\rightarrow$ Sm C_α* $\rightarrow$ (74.6 °C)$\rightarrow$ Sm C* $\rightarrow$ (72.5 °C)$\rightarrow$ Sm C_γ* $\rightarrow$ (70.5 °C)$\rightarrow$ Sm C_A*(−10°C) $\rightarrow$ Cryst. Here, Sm C_A*, Sm C_γ*, and Sm C* denote the AF, FI, and FO phases, respectively. The Sm C_α* phase is one of the intriguing phases whose structure is not clearly understood yet.

The sample cell was made with conductive indium-tin-oxide coated glasses which were treated with polyimides. The polyimide layer was about 300 Å thick. For uniform planar alignment, only one surface of the cell was unidirectionally rubbed. The cell gap was maintained by glass spacers of 5 μm thick, and the effective electrode area was 0.64×0.64 cm^2. The material was filled in the isotropic state and cooled down to the mesophase at a rate of 0.1° C/min. For uniform alignment of both the molecules and the smectic layers, a square wave voltage was applied in the vicinity of the Sm A-Sm C_α* phase transition.

For measuring the electro-optic (EO) transmittance and the switching time near the AF-FO phase transition, the sample cell was placed between cross polarizers such that the AF state produces the minimum transmittance through it. The light

source was a He-Ne laser of 632.8 nm. The applied voltage was generated from an arbitrary waveform generator. The EO transmittance was measured with a digitizing oscilloscope and a digital multimeter.

RESULTS AND DISCUSSION

Fig. 1 shows the EO response to various pulsed electric fields of 0.5 Hz as a function of time at $T = 50°C$. In the absence of the electric field, the minimum transmittance is obtained under crossed polarizers when one of them coincides with the layer normal.

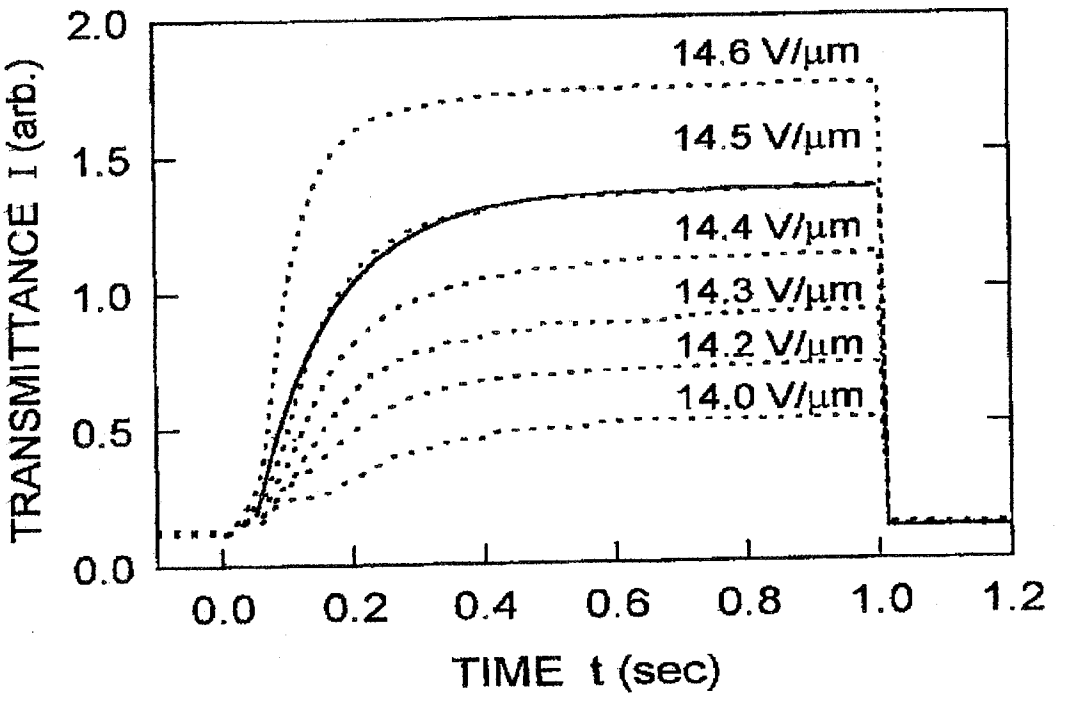

Figure 1: The EO response to various pulsed electric fields of 0.5Hz as a function of time at $T = 50°C$. The solid line at $E = 14.5 V/\mu m$ is a least-square fit to $I = I_0[1 - \exp(-t/\tau_r)]$.

It was found that the AF state responds to the electric field E above a certain threshold E_{th} ($\approx$ 13.8 V/μm). The EO transmittance gradually increases with increasing E. From the least-square fits of the transmittance to a form of $I = I_0[1 - \exp(-t/\tau_r)]$ with the maximum value I_0 and the rising time τ_r, the field induced AF-FO transition can be described in terms of two parameters, I_0 and τ_r. Fig. 2 shows the maximum transmittance I_0 as a function of the field E at several

different temperatures. Note that the maximum transmittance was normalized at each temperature. As shown in Fig. 2, the threshold E_{th} for the AF-FO transition becomes lower at higher temperature T, meaning that the stability of the AF phase decreases with increasing temperature. As reported previously,[5] two processes, one of which is slow and the other is fast, are involved. Below E_{th}, the fast process, associated with a pretransitional effect, gives the transmittance proportional to E^2. Above E_{th}, the slow one corresponding to the field induced molecular reorientation plays a role in the AF-FO phase transition.

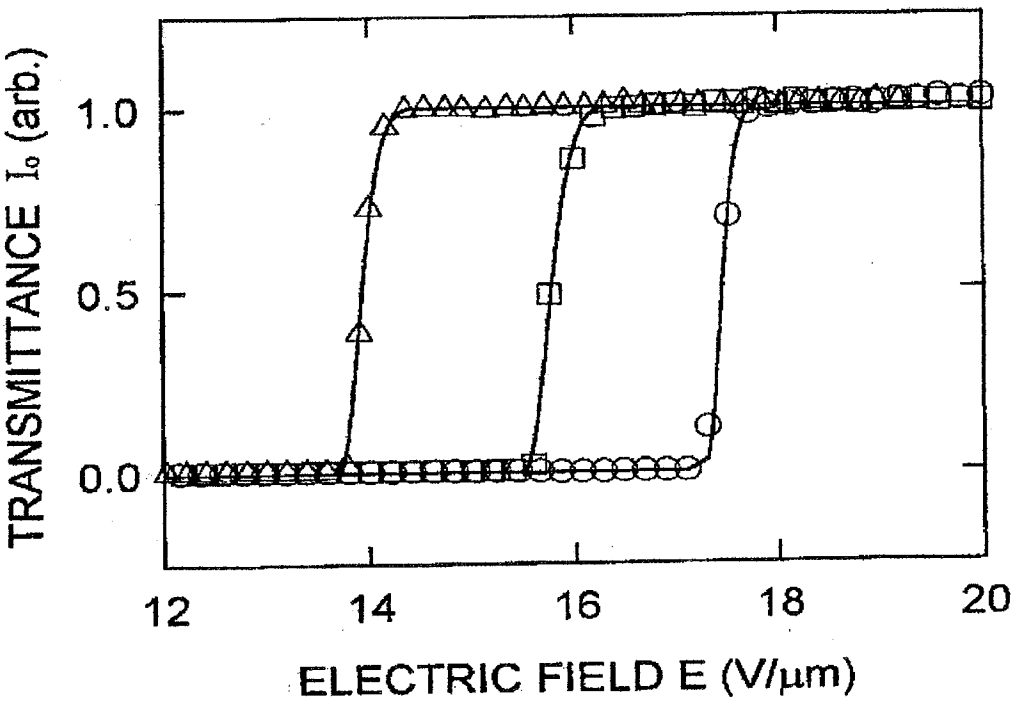

Figure 2: Normalized transmitted intensity I as a function of the electric field E. The open circles, squares, and triangles represent 30°C, 40°C, and 50°C, respectively.

In our study, we will focus ourselves on the slow process such that the cone angle is assumed to remain constant, independent of E, for fixed temperature. One interesting point is that the transmittance has a finite slope which depends on temperature with increasing $E > E_{th}$. This is an indicative of an intermediate state between the AF and FO phase, most likely identified as a FI-like phase. We will discuss this FI ordering along with the anomaly in the rising time τ_r as shown in Fig. 3.

In Fig. 3, the rising time τ_r for the field induced transition from the AF state

to the FO one is shown as a function of the field E at various temperatures. Note that τ_r comes essentially from the slow process. The contribution of the fast one is negligible in the time scale we studied. As shown in Fig. 3, it is clear that τ_r exhibits an anomaly in a certain range of the field E. In this range of E, τ_r reaches a local maximum and then decays exactly as in the FO phase with further increasing E. This resembles the slope of the transmittance I_0 in Fig. 1 in the same range of E.

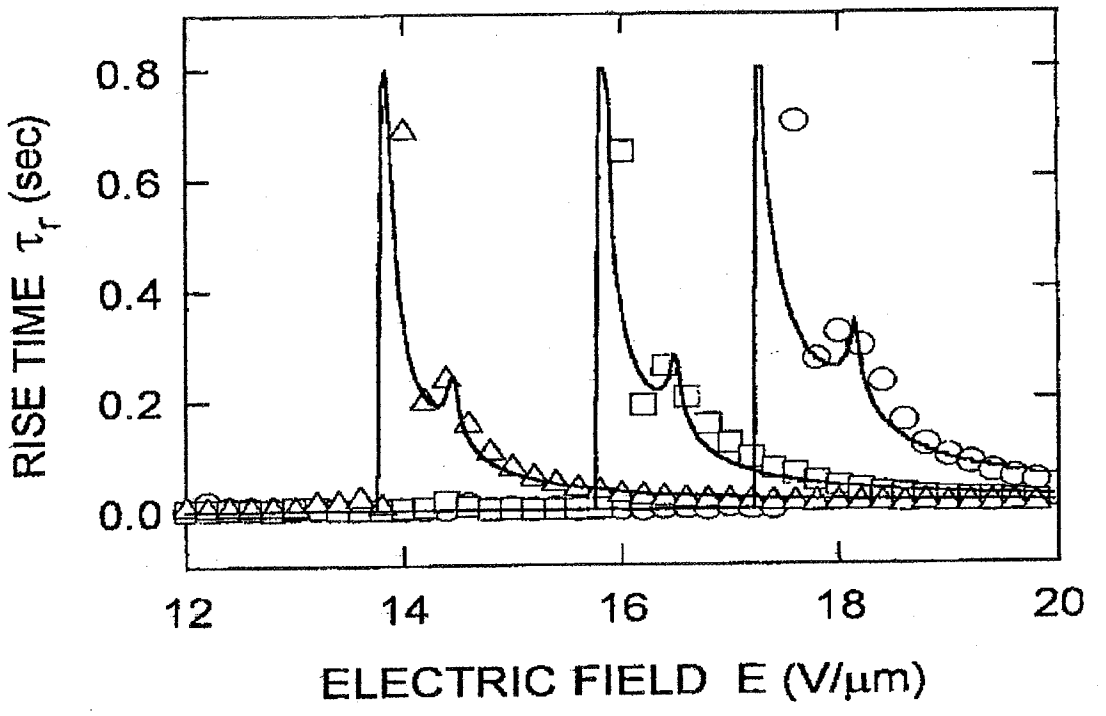

Figure 3: The rising time as a function of the electric field E. The circles, squares, and triangles represent 30°C, 40°C, and 50°C, respectively.

We first construct the free energy of the system to describe the field dependence of the EO transmittance I_0 and the anomaly observed in τ_r. It is assumed that the cone angle does not significantly vary with the electric field E for fixed temperature T. For CS4000, the cone angle $\theta = 27°$. The transverse dipoles of the molecules lie in the plane of the smectic layers. In a bookshelf geometry of the AF phase, the molecules will be inclined at an angle of $\theta/2$ to the layer normal but oppositely in two adjacent layers as shown in Fig. 4. The dipoles in the two layers are then antiparallel to each other. For high fields enough to overcome the pairing of the dipoles in two adjacent layers, the dipoles opposite to the field will reorient to find

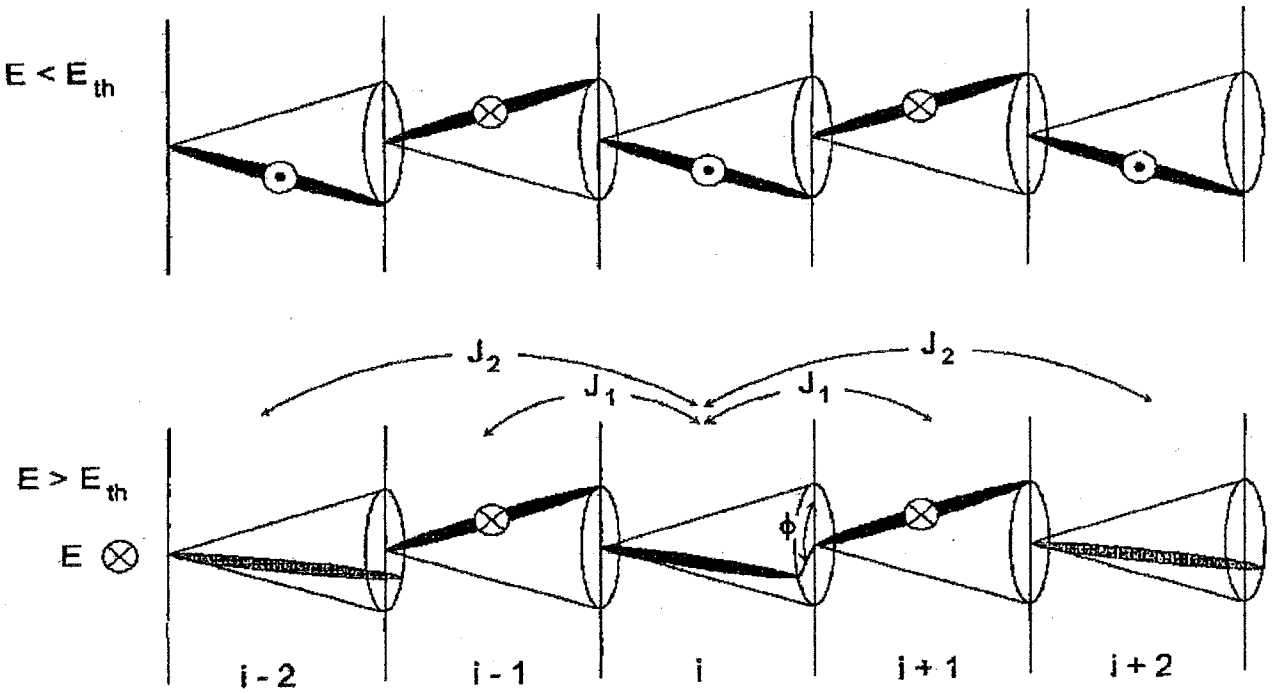

Figure 4: The molecular reorientation under an electric field E. The upper one shows the herringbone structure for $E < E_{th}$ near the AF-FO transition. The lower one shows the molecular reorientation for $E \geq E_{th}$. The angle between two dipoles present in adjacent neighboring layers is denoted by ϕ. J_1 and J_2 represent the layer coupling constants between the N and NN neighboring layers, respectively.

a stable configuration on the cone as shown in Fig. 4.

Let ϕ_i be the azimuthal angle of the dipole in the i-th layer with respect to the field E. The free energy including the interactions of both the N and NN neighboring layer pairs is given by

$$\begin{aligned} G &= \sum_i^M [F_0 + \frac{1}{2}J_1\{\cos(\phi_{i+1} - \phi_i) + \cos(\phi_i - \phi_{i-1})\} \\ &+ \frac{1}{2}J_2\{\cos(\phi_{i+2} - \phi_i) + \cos(\phi_i - \phi_{i-2})\}] - \sum_i^M \vec{P}_i \cdot \vec{E}, \end{aligned} \tag{1}$$

where F_0 the free energy of the FO phase which is independent of ϕ, and P_i the effective polarization in the i-th layer. J_1 and J_2 are the coupling constants between the N and NN neighboring layer pairs, respectively. Here, M denotes total number of layers in the system. Note that fixed boundary conditions will be employed so that surface energies are not introduced in Eq. (1). Under an external electric

field, the dipoles in the NN neighboring layers, the i-th and $(i \pm 2)$-th layers in Fig. 4, will rotate oppositely by the same azimuthal angle to find a minimum energy configuration. The dipoles in the $(i \pm 1)$-th layers will stay as before until the field direction is changed.

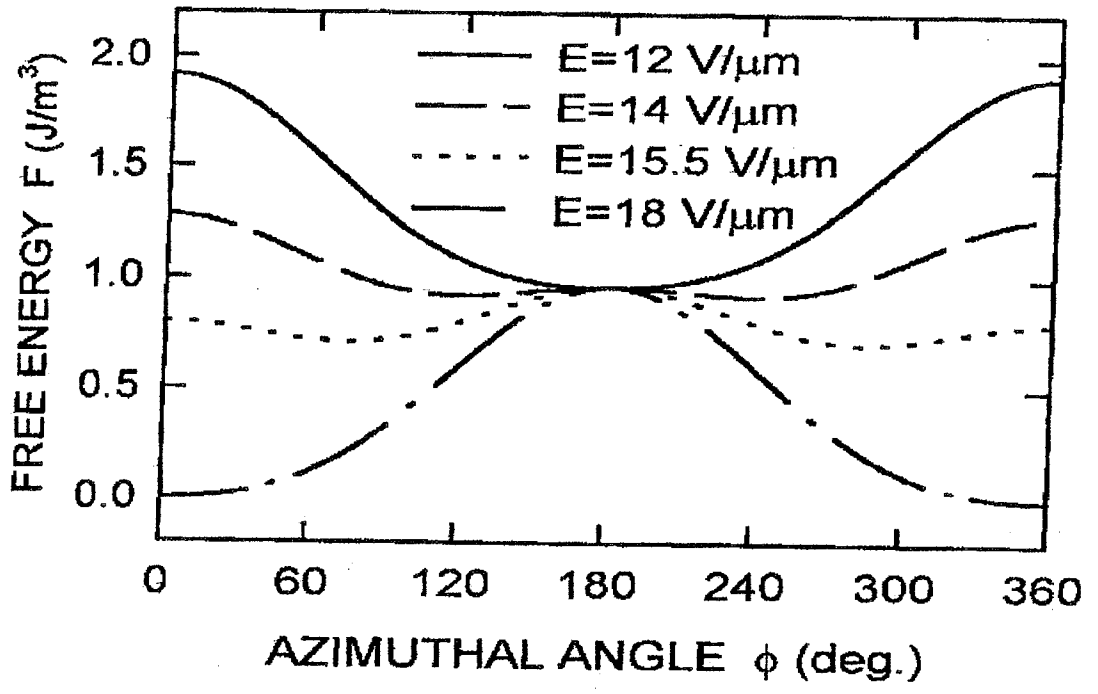

Figure 5: Free energy as a function of the azimuthal angle ϕ at various electric fields.

Assuming that $P_i \equiv P_0$ and $\phi \equiv (\phi_{i+1} - \phi_i)$ for all smectic layers, the free energy per layer can be rewritten as

$$F \equiv \frac{G}{M} = F_0 + J_1 \cos\phi + \frac{1}{2} J_2 (1 + 2\cos 2\phi) - \frac{1}{2} P_0 E (1 + \cos\phi). \qquad (2)$$

The free energy above is shown as a function of ϕ in Fig. 5 at various electric fields. Clearly, the free energy has a minimum at $\phi = \pi$ in low field regime which corresponds to the AF state. As the field increases, this stable state becomes to change from $\phi = \pi$ to $\phi = 0$ (or $\phi = 2\pi$) which represents the FO one. Between the AF and FO states ($0 \leq \phi \leq \pi$ or $\pi \leq \phi \leq 2\pi$), there exists an intermediate FI-like phase. Our experimental results indicate that the AF-FO transition will undergo through the FI-like ordering.

Minimizing the free energy with respect to ϕ, we have

$$\phi = \begin{cases} 0 & \text{for FO,} \\ \cos^{-1}[(P_0E - 2J_1)/4J_2] & \text{for FI,} \\ \pi & \text{for AF.} \end{cases} \tag{3}$$

The FI order will exist in the range of $E_{th} < E < E_c$ where $E_{th} = (2J_1 - 4J_2)/P_0$ and $E_c = (2J_1 + 4J_2)/P_0$. The molecules in the AF state will rearrange themselves at E_{th} and the FO phase appears at E_c through the intermediate FI order.

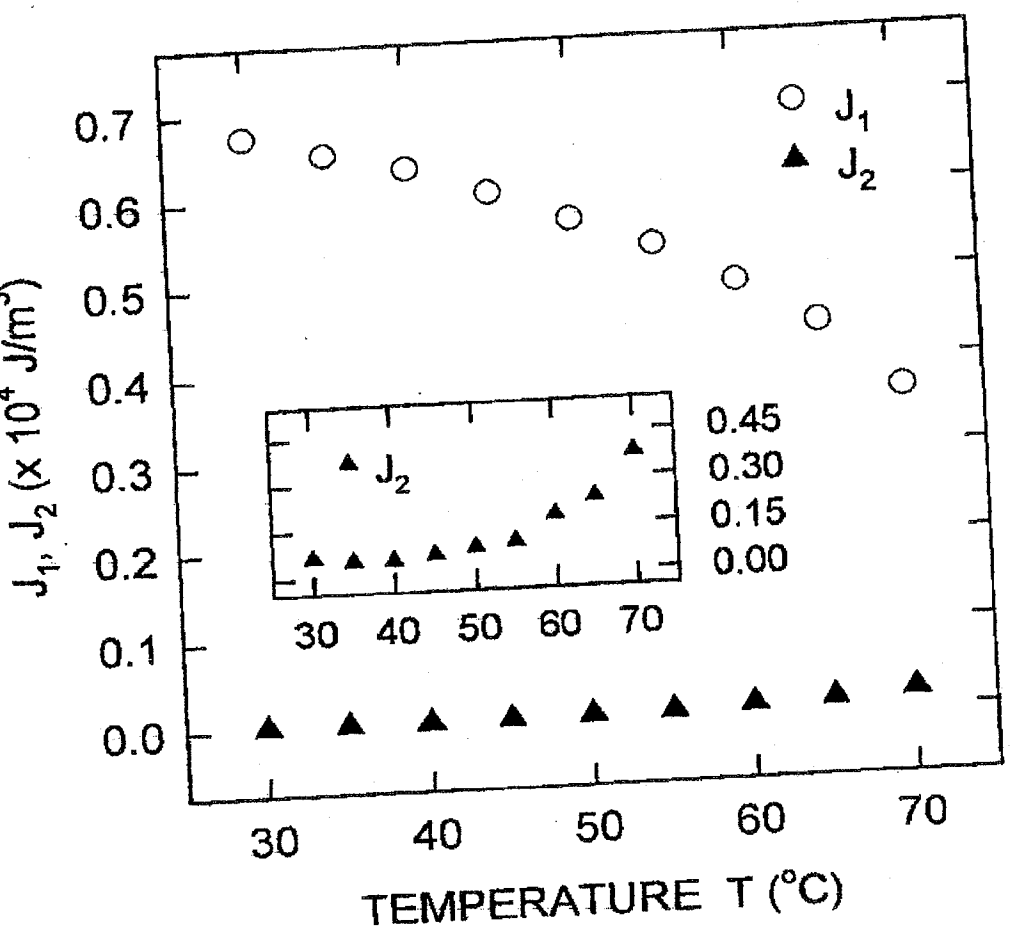

Figure 6: Coupling constants of the N and NN neighboring layer pairs, J_1 and J_2, as a function of temperature T.

During the field induced AF-FO transition described above, the EO transmittance is determined by the average optic axis of the system. The normalized transmittance through the cell is then given by[13] $I/I_0 = \sin^2 2\theta_t$ where $\theta_t = \tan^{-1}(\tan\theta\cos\phi)$. Here, $\theta = 27°$ for CS4000 and ϕ can be obtained from Eq. (3). The solid lines

shown in Fig. 3 are the least-square fits to the above formula. From the best fits, the coupling constants of the N and NN neighboring layer pairs, J_1 and J_2, can be determined at various temperatures. As shown in Fig. 6, J_1 and J_2 determined from I_0 agree well with those from τ_r.

Now, let us examine the effect of the coupling constants, J_1 and J_2, on the field induced AF-(FI)-FO transition. The relative magnitude of J_1 to J_2 is of the order of $(10 \sim 100)$. As the temperature T increases, J_1 decreases monotonically while J_2 increases rather sharply. This suggests that a competition of the layer coupling between the N and NN neighboring pairs is closely related to the intermediate FI ordering. Using the relation of $J_1 \propto \mu_{eff}^2/d^3$ and the measured value of J_1, the magnitude of the dipole moment of an individual molecule can be estimated. Here, μ_{eff} is an effective dipole moment, resulting from the restricted rotation of the molecule around its long axis, and d is the distance between two neighboring dipoles. For DOBAMBC, μ_{eff} is typically 0.1 Debye in the FO phase, depending on the degree of polar ordering.[16,17]

For CS4000, μ_{eff} is estimated as about 1.3 Debye from $J_1 = 7.0 \times 10^3$ J/m^3 at $T = 30$°C provided that $d \approx 30\mathring{A}$ and $\rho \approx 10^{27}$/m^3 for the number density.[16,18] This estimated μ_{eff} is about ten times larger than that for DOBAMBC. Since the polar order was found to be about 0.1 for DOBAMBC,[17] the transverse molecular dipole moment $\mu_{FLC} \simeq 1$ Debye. Taking the same degree of the polar order for most AFLCs, $\mu_{AFLC} \simeq 13$ Debye.[7] This is not physically unreasonable since the molecules for the AF ordering are believed to possess significantly large transverse dipole moments on the end chains.

We now discuss the anomaly in τ_r in Fig. 3 within the framework of Eq. (1). The dynamic equation derived from the free energy is given by

$$\gamma \frac{\partial \phi}{\partial t} = -(\frac{1}{2} P_0 E - J_1 - 2J_2 \cos\phi)\sin\phi, \tag{4}$$

where γ is the relevant viscosity. By performing numerical simulations, based on Eq. (4), the temporal profiles of the azimuthal angle ϕ is obtained for given field E. In a certain range of E, the relaxation rate of ϕ was found to decrease in time, which gives the anomaly shown in Fig. 3. The solid lines in Fig. 3 represent theoretical fits obtained from numerical simulations with the help of the measured J_1 and J_2. Clearly, the experimental results for both I_0 and τ_r can be explained self-consistently within the framework of our model. Qualitatively, the competition between the N and NN neighboring pair interactions results in the anomaly in τ_r in terms of the FI-like ordering. For the azimuthal angle of $\pi/2 \leq \phi < \pi$, the NN interaction will

be repulsive while the N one will be attractive. For the angle of $0 \leq \phi < \pi/2$, both N and NN interactions are repulsive, so that τ_r increases. The effect of J_2 on the anomaly in τ_r is clearly shown in Fig. 7. Interestingly, for $J_2 = 0$, no anomalous peak of τ_r can be observed, and for finite J_2, it moves to a higher field region with increasing J_2.

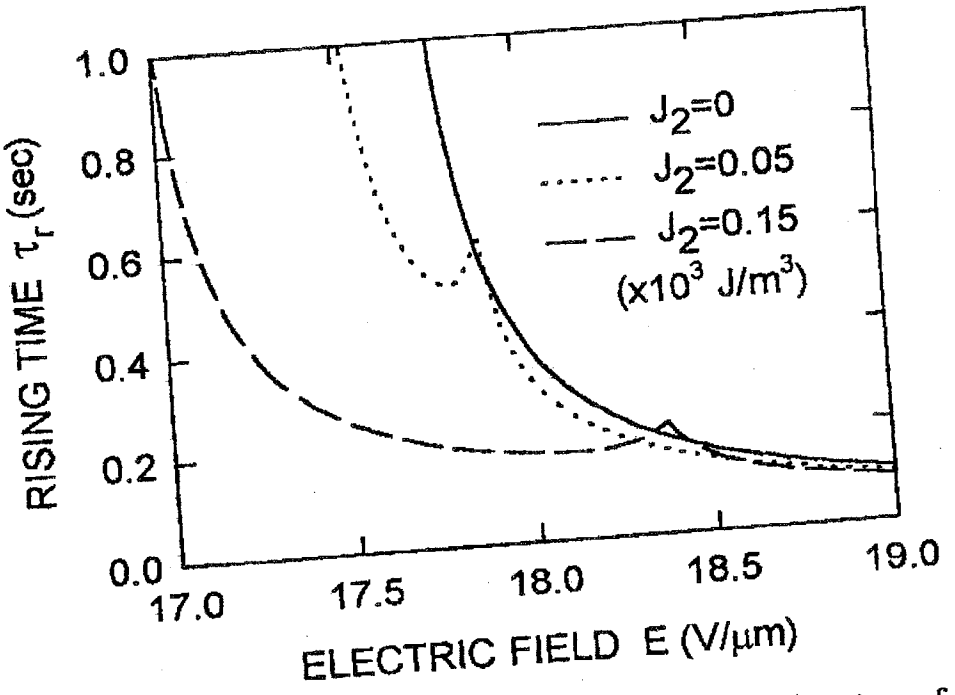

Figure 7: The effect of J_2 on the anomaly in τ_r as a function of the field E for $J_1 = 7.0 \times 10^3$ J/m^3.

It is also noted that the slope of the transmittance I_0 during the field induced AF-(FI)-FO transition becomes steeper as J_2 decreases. However, J_1 affects only the threshold for the AF-(FI)-FO transition in such a way that the threshold becomes larger with increasing J_1. For practical applications, it may be desirable to design AFLC materials with appropriate values of J_1 and J_2 which represent the layer coupling of the N and NN neighboring layer pairs.

CONCLUDING REMARKS

We have presented experimental results for the layer coupling of the N and NN neighboring layers near the field induced AF-(FI)-FO transition. The relative magnitude of the layer coupling of N pairs to the NN pairs was found to be in the range of

($10 \sim 100$), depending on the degree of the polar order. The dipole moment of an individual molecule for the AF ordering is about ten times larger than that for typical FLCs. It was found that the interactions between the NN neighboring layer pairs play a critical role in describing the anomaly observed in the switching time. This anomaly is an indicative of the existence of an intermediate FI-like ordering.

ACKNOWLEDGEMENT

This work was supported in part by KOSEF through RCDAMP at Pusan National University.

REFERENCES

1. A. D. L. Chandani, T. Hagiwara, Y. Ouchi, H. Takezoe, and A. Fukuda, Jpn. J. Appl. Phys. 27, L729 (1988).
2. E. Gorecka, A. D. L. Chandani, Y. Ouchi, H. Takezoe, and A. Fukuda, Jpn. J. Appl. Phys. 29, 131 (1990).
3. I. Muševič, B. Žekš, R. Blinc, and T. Rasing, Phys. Rev. E 47, 1094 (1993).
4. J. Philip, J. R. Lalanne, J. P. Marcerou, and G. Sigaud, Phys. Rev. E 52, 1846 (1995).
5. M. Johno, K. Itoh, J. Lee, Y. Ouchi, H. Takezoe, A. Fukuda, and T. Kitazume, Jpn. J. Appl. Phys. 29, L107 (1990).
6. K. Hiraoka, A. Taguchi, Y. Ouchi, H. Takezoe, and A. Fukuda, Jpn. J. Appl. Phys. 29, L103 (1990).
7. A. Fukuda, Y. Takanishi, T. Isozaki, K. Ishikawa, and H. Takezoe, J. Mater. Chem. 4, 997 (1994).
8. Y. Takanishi, K. Hiraoka, V. K. Agrawal, H. Takezoe, A. Fukuda, and M. Matsushita, Jpn. J. Appl. Phys. 30, 2023 (1991).
9. K. Hiraoka, A. D. L. Chandani, E. Gorecka, Y. Ouchi, H. Takezoe, and A. Fukuda, Jpn. J. Appl. Phys. 29, L1473 (1990).
10. J. Hatano, M. Harazaki, M. Sato, K. Iwauchi, S. Saito, and K. Murashiro, Jpn. J. Appl. Phys. 32, 4344 (1993).
11. M. Nakagawa, Jpn. J. Appl. Phys. 30, 1759 (1991).
12. N. Yamamoto, Y. Yamada, K. Mori, K. Nakamura, H. Orihara, Y. Ishibashi, Y. Suzuki, Y. Negi, and I. Kawamura, Jpn. J.Appl. Phys. 30, 2380 (1991).
13. H. Pauwels, A. De Meyere, and J. Fornier, Mol. Cryst. Liq. Cryst. 263, 469 (1995).
14. H. Hayashi, M. Takemura, K. Kikuchi, K. Takigawa, M.Inata, Y. Hijikata, K. Ezaka, H. Shindo, H. Orihara, and Y. Ishibashi, Jpn. J. Appl. Phys. 34, 5438 (1995).
15. J.-H. Kim and S.-D. Lee (unpublished results)

16. J. W. Goodby et al., Ferroelectric Liquid Crystals; Principles, Properties, and Applications (Gordon and Breach Science, Philadelphia, 1991).
17. J. Seliger, V. Žagar, and R. Blinc, Phys. Rev. A 17, 1149 (1978).
18. A. Suzuki, H. Orihara, Y. Ishibashi, Y. Yamada, N. Yamamoto, K. Mori, K. Nakamura, Y. Suzuki, T. Hagiwara, I. Kawamura, and M. Fukui, Jpn. J. Appl. Phys. 29, L336 (1990).